

Effects of energy dependent spacetime on geometrical thermodynamics and heat engine of black holes: gravity's rainbow

B. Eslam Panah^{1,2*}

¹ *Research Institute for Astronomy and Astrophysics of Maragha (RIAAM), P.O. Box 55134-441, Maragha, Iran*

² *ICRANet, Piazza della Repubblica 10, I-65122 Pescara, Italy*

Inspired by applications of gravity's rainbow in UV completion of general relativity, we investigate charged topological black holes in gravity's rainbow and show that depending on the values of different parameters, these solutions may encounter with black hole solutions with two horizons, extreme black hole (one horizon) or naked singularity (without horizon). First, we obtain black hole solutions, calculate thermodynamical quantities of the system and check the first law of thermodynamics. Then, we study the thermodynamical behavior of the system including thermal stability and phase transitions. In addition, we employ geometrical thermodynamics to probe phase transition points and limits on having physical solutions. Finally, we obtain heat engines corresponding to these black holes. The goal is to see how black holes' parameters such as topological factor and rainbow functions would affect efficiency of the heat engines.

I. INTRODUCTION

Since the introduction of general relativity, there has been an ongoing attempt to modify gravity at the fundamental level. To name a few, one can point out to Lovelock gravity [1, 2], brane world cosmology [3, 4], scalar-tensor theories [5, 6], $F(R)$ gravity [7–10], massive gravity [11–13], and also gravity's rainbow [14, 15]. Among these modifications of Einstein gravity, gravity's rainbow seems to be a promising candidate in dealing with Ultra-Violet divergences (UV).

To introduce gravity's rainbow, one should first understand the concepts of doubly special relativity. In special relativity, an upper limit of the velocity of light is imposed on particles' velocities. Following the same principle, one can also consider an upper limit on energy of the particles as well. This upper limit is the Planck energy. In the literature, this is called doubly special relativity (DSR) [16–19]. Indeed, DSR is an extension of special relativity where there are two fundamental upper bounds on properties of particles: the velocity of light and Planck energy. The DSR is in the non-curved space. If we generalize such theory to curved spacetime and include the gravity, we will have doubly general relativity or gravity's rainbow [14, 15]. In gravity's rainbow, the test particles with various energy experience the gravity differently. In other words, gravity has an effective behavior on particles determined by their energy. Going back to DSR, in order to incarnate the upper limit on energy particles, one should use a nonlinear Lorentz transformation in momentum space. This implies a deformed Lorentz symmetry such that the usual dispersion relation in special relativity may be modified by Planck scale correction. It should be noted that it was speculated that the Lorentz infraction or deformation may be an essential property in constructing a quantum theory of gravity.

The modified version of the energy-momentum dispersion is given by

$$E^2 f^2(E/E_p) - p^2 g^2(E/E_p) = m^2 \quad (1)$$

where m and E are mass and energy of a test particle, respectively. Also E_p is the Planck energy scale. For simplicity, we rename the following ratio $\varepsilon = E/E_p$. The value of this ratio is always less than one, because the energy of a test particle can not be larger than the Planck energy [20]. The functions $f(\varepsilon)$ and $g(\varepsilon)$ are called rainbow functions and satisfy the following equation

$$\lim_{\varepsilon \rightarrow 0} f(\varepsilon) = 1, \quad \lim_{\varepsilon \rightarrow 0} g(\varepsilon) = 1, \quad (2)$$

these limits are originated from infrared (IR) limit where the usual general relativity must be recovered. Studies conducted with consideration of gravity's rainbow proven to be fruitful. Among the achievements of gravity's rainbow, one can point to providing possible solutions for information paradox [21, 22], absence of black hole production at LHC [23], and the existence of remnants for black holes after evaporation [24]. Cosmologically speaking, consideration of gravity's rainbow could remove the big bang singularity [25–27]. Also the initial singularity problem [28] and stability of Einstein static universe in gravity's rainbow have been studied [29]. In the context of astrophysics, it was shown

* email address: behzad.eslampanah@gmail.com

that the maximum mass of neutron stars [30, 31] and white dwarfs [32] in the presence of gravity's rainbow, are an increasing function of rainbow functions (see Refs. [33, 34], for another properties of neutron stars and white dwarfs). In the context of gravity, it was pointed out that Horava-Lifshitz gravity can be related to the gravity's rainbow through suitable scaling for the energy functions [35]. In the context of black holes, several studies focusing on effects of gravity's rainbow on thermodynamics of black holes in general relativity were done in Refs. [36–42]. The influence of gravity's rainbow to the global Casimir effect around a static mini black hole at zero and finite temperature has been studied in Ref. [43]. Consideration of gravity's rainbow with modified gravity such as $F(R)$ theories of gravity [44, 45], massive gravity [46], Gauss–Bonnet gravity [47, 48], Lovelock gravity [49], and also, dilaton gravity [50] were also done.

Among the different solutions in gravity, the black holes have been an interesting subject that have attracted a lot of attention over past 100 years old. The discovery of the gravitational waves on one hand and thermodynamical properties of the black holes on the other hand [51–53], have made black hole an interesting platform for investigating the nature of gravity. In addition, the introduction of the adS/CFT duality and string theory inspired applications of the black holes provided more reasons to investigate the black holes [54–59]. Considering these issues, we study black hole solutions in gravity's rainbow here.

Among the recent thermodynamical advances in the field of black holes thermodynamics, one can point out to extended phase space and geometrical thermodynamics. In the extended phase space, one consider the cosmological constant in adS black holes to be a thermodynamical quantity known as pressure [60, 61]. Such consideration results into introduction of a van der Waals behavior, the reentrant of phase transition [62, 63], existence of the triple point [64, 65] and possibility of having classical heat engine [66, 67, 70–82]. The geometrical thermodynamics approach uses the thermodynamical quantities to built a metric which describes thermal phases of the corresponding black hole [84–90]. The thermodynamical behavior is understood by Ricci scalar of the metric. Changes in Ricci scalar's sign and its divergencies are employed to depict the thermal phases of black holes in this approach. The aim is to have thermodynamical structure of the black holes described by Riemannian calculus. So far, different methods are proposed for constructing the thermodynamical metric which among them, one can point out to Weinhold [84, 85], Ruppeiner [86, 87], Quevedo [88, 89] and HPEM [90].

In this paper, we intent to investigate thermodynamical properties of the black holes in the presence of gravity's rainbow. Here, we address the modifications imposed on thermal stability conditions and possible bounds on having physical solutions. In addition, we regard geometrical thermodynamic approach to investigate phase transitions of the solutions. Next, we construct heat engines inspired by these black holes and show how the rainbow functions would modify the efficiency of these engines. The paper will be concluded by some closing remarks.

II. BLACK HOLES IN GRAVITY'S RAINBOW

Here, we start with the 4-dimensional action of Einstein gravity in the presence of cosmological constant which depends on the energy $(\Lambda(\varepsilon))$ with an abelian $U(1)$ gauge field as

$$I = -\frac{1}{16\pi G(\varepsilon)} \int d^4x \sqrt{-g} (R - 2\Lambda(\varepsilon) - F), \quad (3)$$

where R is the scalar curvature. $F = F_{\mu\nu}F^{\mu\nu}$ is the Maxwell invariant, in which $F_{\mu\nu} = \partial_\mu A_\nu - \partial_\nu A_\mu$ is the Faraday tensor, and also A_μ is the gauge potential.

Variation of the action (3) with respect to the metric $(g_{\mu\nu})$ and the Faraday tensors $(F_{\mu\nu})$ leads to the following field equations

$$G_{\mu\nu}(\varepsilon) + \Lambda(\varepsilon)g_{\mu\nu} = 8\pi G(\varepsilon)T_{\mu\nu}, \quad (4)$$

$$\nabla_\mu F^{\mu\nu} = 0, \quad (5)$$

where

$$T_{\mu\nu} = 2F_{\mu\lambda}F_\nu^\lambda - \frac{1}{2}g_{\mu\nu}F, \quad (6)$$

$G_{\mu\nu}(\varepsilon)$ is Einstein's tensor which is assumed to be energy dependent. Since we are working in natural units, we set $8\pi G(\varepsilon) = 1$.

We consider a topological 4-dimensional static energy dependent spacetime with the following form

$$ds^2 = -\frac{\psi(r, \varepsilon)}{f^2(\varepsilon)} dt^2 + \frac{1}{g^2(\varepsilon)} \left[\frac{dr^2}{\psi(r, \varepsilon)} + r^2 d\Omega^2 \right], \quad (7)$$

where $\psi(r, \varepsilon)$ is the metric function. Also, in the above equation, $d\Omega^2$ is given by

$$d\Omega^2 = \begin{cases} d\theta^2 + \sin^2 \theta d\varphi^2 & k = 1 \\ d\theta^2 + d\varphi^2 & k = 0 \\ d\theta^2 + \sinh^2 \theta d\varphi^2 & k = -1 \end{cases}, \quad (8)$$

It is notable that the constant k indicates that the boundary of $t = \text{constant}$ and $r = \text{constant}$ can be elliptic ($k = 1$), flat ($k = 0$) or hyperbolic ($k = -1$) curvature hypersurface.

In order to obtain electrically charged black holes in gravity's rainbow, we consider a radial electric field which its related gauge potential is in the following form

$$A_\mu = h(r, \varepsilon) \delta_\mu^t. \quad (9)$$

Using the metric (7) with the Maxwell equations (5), we can find the following differential equation

$$r h''(r, \varepsilon) + 2h'(r, \varepsilon) = 0, \quad (10)$$

in which the prime and double prime, respectively, are the first and the second derivatives with respect to r . One finds the solution of the equation (10) as

$$h(r, \varepsilon) = -\frac{q(\varepsilon)}{r}, \quad (11)$$

where $q(\varepsilon)$ is a parameter which is related to the electric charge. It is worthwhile to mention that the electromagnetic field tensor is $F_{tr} = \partial_t A_r - \partial_r A_t = \frac{q(\varepsilon)}{r^2}$, which depends on the energy-dependent electrical charge ($q(\varepsilon)$) and r .

Considering the introduced metric (7) and the field equations (4), we want to obtain exact solutions for the metric function $\psi(r, \varepsilon)$. We obtain the following differential equations

$$eq_{tt} = eq_{rr} = g^2(\varepsilon) [r^3 \psi'(r, \varepsilon) + r^2 (\psi(r, \varepsilon) - k) + q^2(\varepsilon) f^2(\varepsilon)] + \Lambda(\varepsilon) r^4, \quad (12)$$

$$eq_{\theta\theta} = eq_{\varphi\varphi} = g^2(\varepsilon) [2r^3 \psi'(r, \varepsilon) + r^4 \psi''(r, \varepsilon) - 2q^2(\varepsilon) f^2(\varepsilon)] + 2\Lambda(\varepsilon) r^4, \quad (13)$$

where eq_{tt} , eq_{rr} , $eq_{\theta\theta}$ and $eq_{\varphi\varphi}$ are components of tt , rr , $\theta\theta$ and $\varphi\varphi$ of field equation (4), respectively. Considering eqs. (12) and (13), after some calculations, one can obtain the following metric function

$$\psi(r, \varepsilon) = k - \frac{m_0(\varepsilon)}{r} - \frac{\Lambda(\varepsilon) r^2}{3g^2(\varepsilon)} + \frac{q^2(\varepsilon) f^2(\varepsilon)}{r^2}, \quad (14)$$

where $m_0(\varepsilon)$ is integration constant related to the total mass of the black hole.

In order to investigate the geometrical structure of these solutions, we first look for the essential singularity(ies). The Ricci and Kretschmann scalars can be written as

$$R = 4\Lambda(\varepsilon) \quad (15)$$

$$R_{\mu\nu\lambda\kappa} R^{\mu\nu\lambda\kappa} = \frac{8\Lambda^2(\varepsilon)}{3} + \frac{12m_0^2(\varepsilon)g^4(\varepsilon)}{r^6} - \frac{48m_0(\varepsilon)q^2(\varepsilon)f^2(\varepsilon)g^2(\varepsilon)}{r^7} + \frac{56q^4(\varepsilon)f^4(\varepsilon)g^4(\varepsilon)}{r^8}, \quad (16)$$

where our calculations confirm that, there is a curvature singularity at $r = 0$ ($\lim_{r \rightarrow 0} R_{\mu\nu\lambda\kappa} R^{\mu\nu\lambda\kappa} \rightarrow \infty$), and also the asymptotical behavior of this spacetime is (anti)de Sitter ((a)dS) at $r \rightarrow \infty$ ($\lim_{r \rightarrow \infty} R_{\mu\nu\lambda\kappa} R^{\mu\nu\lambda\kappa} = \frac{8\Lambda^2(\varepsilon)}{3}$). It is worthwhile to mention that the asymptotical behavior of obtained solutions is energy dependent. On the other hand, by replacing $f(\varepsilon) = g(\varepsilon) = 1$, the solution (14) reduces to topological Reissner–Nordström black hole solutions in (a)dS spacetime, namely, $\psi(r) = k - \frac{m_0}{r} - \frac{\Lambda r^2}{3} + \frac{q^2}{r^2}$. In order to investigate the possibility of the horizon, we study the behavior of obtained metric function (14) versus r in Fig. 1. We found that the presented solutions may be interpreted as black hole solutions with two horizons (inner and outer horizons), extreme black hole (one horizon) or naked singularity (without horizon).

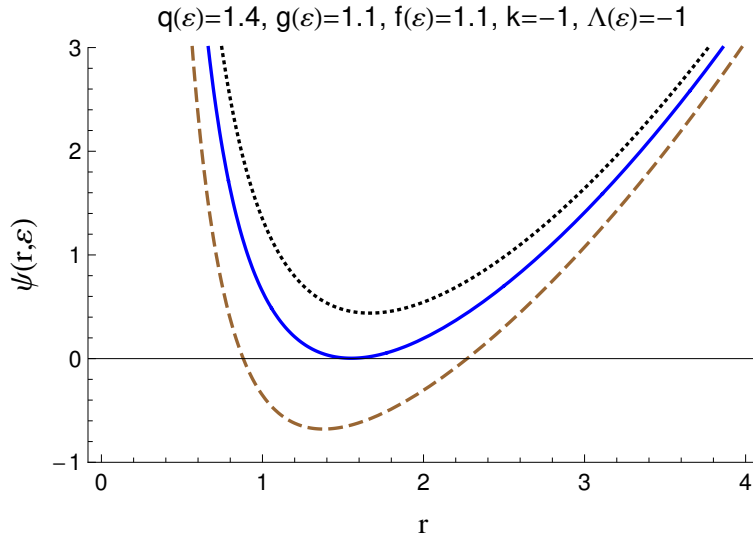


FIG. 1: $\psi(r, \varepsilon)$ versus r for $m_0(\varepsilon) = 0.3$ (dotted line), $m_0(\varepsilon) = 1.0$ (continuous line) and $m_0(\varepsilon) = 2.0$ (dashed line).

III. THERMODYNAMICS

In this section, we want to calculate the conserved and thermodynamic quantities, and check the first law of thermodynamics for these black holes.

Considering the metric (7) and the obtained black hole solutions (14), the Hawking temperature of these black holes can be derived from the definition of surface gravity at the outer horizon r_+ as follows [91, 92]:

$$T = \frac{g(\varepsilon)}{4\pi f(\varepsilon)} \psi'(r, \varepsilon)|_{r=r_+} = \frac{1}{4\pi} \left(\frac{g(\varepsilon) [kr_+^2 - q^2(\varepsilon)f^2(\varepsilon)]}{f(\varepsilon)r_+^3} - \frac{\Lambda(\varepsilon)r_+}{f(\varepsilon)g(\varepsilon)} \right). \quad (17)$$

It is notable that, the dependency on the rainbow functions indicates that the temperature is modified.

The entropy of black holes satisfies the so-called area law of entropy in general relativity. It means that the black hole's entropy equals to one-quarter of horizon area (see Ref. [93]). Therefore, the entropy of black holes is given by

$$S = \frac{r_+^2}{4g^2(\varepsilon)}. \quad (18)$$

The equation (18) shows that, the obtained entropy is modified in gravity's rainbow.

In order to obtain the total charge of these solutions, one can employ the Gauss law. Therefore, one can find the total electric charge in the following form

$$Q = \frac{q(\varepsilon)f(\varepsilon)}{4\pi g(\varepsilon)}. \quad (19)$$

The obtained total charge depends on rainbow functions. In other words, the total charge is modified in this gravity. In order to obtain the electric potential (U), we can calculate it on the horizon with respect to a reference

$$U = A_\mu \chi^\mu|_{r \rightarrow \infty} - A_\mu \chi^\mu|_{r \rightarrow 0} = \frac{q(\varepsilon)}{r_+}. \quad (20)$$

Another important conserved quantity is related to total mass of the black holes. For finding it, one can use Hamiltonian approach which results into

$$M = \frac{m_0(\varepsilon)}{8\pi f(\varepsilon)g(\varepsilon)}. \quad (21)$$

Using the obtained conserved and thermodynamic quantities, we can check the first law of thermodynamics for topological charged black hole solutions in gravity's rainbow. For this purpose, we obtain the mass as a function of

the extensive quantities S and Q . Considering Eqs. (14), (18) and (19) and by replacing them in Eq. (21), the mass $M(S, Q)$ is found as

$$M(S, Q) = \frac{4\Lambda(\varepsilon)S^2 - 3kS - 12\pi^2Q^2}{-12\pi f(\varepsilon)\sqrt{S}}. \quad (22)$$

Now, we define the intensive parameters conjugate to S and Q . These quantities are the temperature and the electric potential

$$T = \left(\frac{\partial M(S, Q)}{\partial S} \right)_Q = \frac{4\Lambda(\varepsilon)S^2 - kS + 4\pi^2Q^2}{-8\pi f(\varepsilon)S^{3/2}}, \quad (23)$$

$$U = \left(\frac{\partial M(S, Q)}{\partial Q} \right)_S = \frac{2\pi Q}{f(\varepsilon)\sqrt{S}}, \quad (24)$$

The results of Eqs. (23), (24) coincide with Eqs. (17) and (20), therefore, we find that these conserved and thermodynamic quantities satisfy the first law of black hole thermodynamics as

$$dM = TdS + UdQ. \quad (25)$$

IV. STABILITY AND GEOMETRICAL THERMODYNAMICS

Here, first, we are going to study the stability of solutions in the context of heat capacity. Next, we consider the geometrical approach for studying phase transitions. We investigate the effects of energy dependent parameters on thermodynamical behavior and compare the results of both approaches.

In context of the canonical ensemble, the heat capacity is one of the thermodynamical quantities carrying crucial information regarding thermal structure of the black holes. The heat capacity includes three specific interesting information. First, the discontinuities of this quantity mark the possible thermal phase transitions that system can undergo. Second, the sign of it determines whether the system is thermally stable or not. Indeed, the positivity corresponds to thermal stability while the opposite shows instability. Third, the roots of this quantity are also of interest since it may yield the possible changes between stable/instable states or bound point. Due to these important points, this section and the following one are dedicated to calculation of the heat capacity of the solutions and investigation of thermal structure of the black holes using such quantity. We will show that by using this quantity alongside of the temperature, we can draw a picture regarding the possible thermodynamical phase structures of these black holes and stability/instability that these black holes could enjoy/suffer. One can calculate the heat capacity in the following form

$$C_Q = T \left(\frac{\partial S}{\partial T} \right)_Q = \frac{\left(\frac{\partial M(S, Q)}{\partial S} \right)_Q}{\left(\frac{\partial^2 M(S, Q)}{\partial S^2} \right)_Q} = \frac{2S [4\Lambda(\varepsilon)S^2 - kS + 4\pi^2Q^2]}{4\Lambda(\varepsilon)S^2 + kS - 12\pi^2Q^2}. \quad (26)$$

In the context of black holes, it is argued that the root of heat capacity ($C_Q = T = 0$) is representing a border line between physical ($T > 0$) and non-physical ($T < 0$) black holes. We call it a physical limitation point. The system in the case of this physical limitation point has a change in sign of the heat capacity. In addition, it is believed that the divergencies of the heat capacity represent phase transition critical points of black holes. Therefore, the phase transition critical and limitation points of the black holes in the context of the heat capacity are calculated with the following relations

$$\begin{cases} T = \left(\frac{\partial M(S, Q)}{\partial S} \right)_Q = 0 & \text{physical limitation points} \\ \left(\frac{\partial^2 M(S, Q)}{\partial S^2} \right)_Q = 0 & \text{phase transition critical points} \end{cases}. \quad (27)$$

In order to find the physical limitation points, we consider Eq. (23) and solve the following equation for the entropy:

$$T = \left(\frac{\partial M(S, Q)}{\partial S} \right)_Q = \frac{4\Lambda(\varepsilon)S^2 - kS + 4\pi^2Q^2}{-8\pi f(\varepsilon)S^{3/2}} = 0. \quad (28)$$

TABLE I: The physical limitation points for $Q = 0.02$.

k	$\Lambda(\varepsilon)$	S_1	S_2	number of points
1	1	0.017	0.233	2
1	-1	0.015	-	1
0	1	-	-	0
0	-1	0.063	-	1
-1	1	-	-	0
-1	-1	0.265	-	1

We find two roots (S_1 and S_2) for the above equation as

$$\begin{cases} S_1 = \frac{k - \sqrt{k^2 - 64\pi^2\Lambda(\varepsilon)Q^2}}{8\Lambda(\varepsilon)} \\ S_2 = \frac{k + \sqrt{k^2 - 64\pi^2\Lambda(\varepsilon)Q^2}}{8\Lambda(\varepsilon)} \end{cases}, \quad (29)$$

In order to have real roots, we should consider $k^2 - 64\Lambda(\varepsilon)\pi^2Q^2 \geq 0$, therefore, $Q \leq \pm \frac{k}{8\pi\sqrt{\Lambda(\varepsilon)}}$. Our results about the physical limitation points (29) show that these points depend on topological factor (k), the cosmological constant ($\Lambda(\varepsilon)$) and also the total charge (Q). Considering the obtained limitation for the total charge ($Q \leq \pm \frac{k}{8\pi\sqrt{\Lambda(\varepsilon)}}$), we investigate the behavior of the physical limitation points in table (I) and figures 2, 3, 4 and 5.

Now, we investigate the obtained physical limitation points in table (I). One should note it that the sign of temperature and heat capacity put a restriction on the system as to it being physical or non-physical and also stable or unstable. In other words, the negativity of temperature and heat capacity is denoted as non-physical and unstable system, whereas the positivity of temperature and heat capacity is denoted as a physical and stable system. Here, our system is black hole.

Our solutions include three different cases for topological charged black holes in gravity's rainbow:

Case I: existence of two roots for the temperature and the heat capacity (Fig. 2). In this case, there are two critical entropy, namely S_1 and S_2 , in which for $S < S_1$, the temperature and the heat capacity of black holes are negative. Therefore, the black holes with small entropy are non-physical and unstable. For $S_2 < S$, the heat capacity is positive but the temperature is negative. Therefore the black holes with large entropy are non-physical. It is notable that, there is an important region which is related to $S_1 < S < S_{div}$, where S_{div} is divergence point. Temperature and heat capacity of black holes in this region are positive. In other words, the obtained black holes are physical and enjoy thermal stability when their entropy is in range $S_1 < S < S_{div}$. Also, for region $S_{div} < S < S_2$, the temperature is positive but the heat capacity is negative. Indeed, the black holes are physical but unstable (see Fig. 2).

Case II: there is a critical entropy, S_1 . Here, we have two different behaviors. First: for $S < S_1$, temperature and heat capacity of the black holes are negative and therefore our systems are non-physical and unstable. But for $S > S_1$, these quantities are positive and therefore our black holes are physical and stable. In other words, our results confirm that the black holes with large entropy are physical and enjoy thermal stability but for small entropy the black holes are non-physical and unstable (see Fig. 3). Second: the temperature and the heat capacity are negative and so the systems are non-physical and unstable in the range $S < S_1$, but for $S > S_1$, the temperature is positive while the heat capacity has different sign (see Fig. 4).

Case III: there is no root. In this case, the temperature of black holes is negative. Although the heat capacity of these black holes may be positive but the temperature of black holes is always negative. In other words, the obtained black holes are non-physical (see Fig. 5).

In order to study the phase transition critical points, we obtain the following relation

$$\left(\frac{\partial^2 M(S, Q)}{\partial S^2} \right)_Q = 4\Lambda(\varepsilon)S^2 + kS - 12\pi^2Q^2 = 0. \quad (30)$$

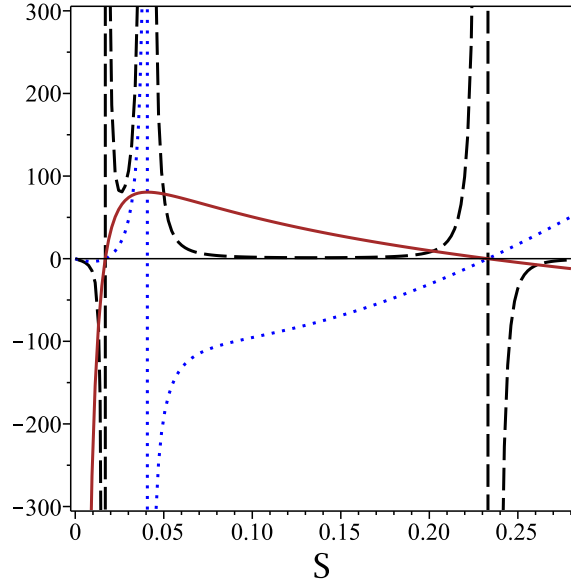


FIG. 2: T (continuous line), C_Q (dotted line) and $R_{HP\text{EM}}$ (dashed line) versus S for $Q = 0.02$, $\Lambda(\varepsilon) = 1$, $f(\varepsilon) = g(\varepsilon) = 1.1$, $k = 1$.

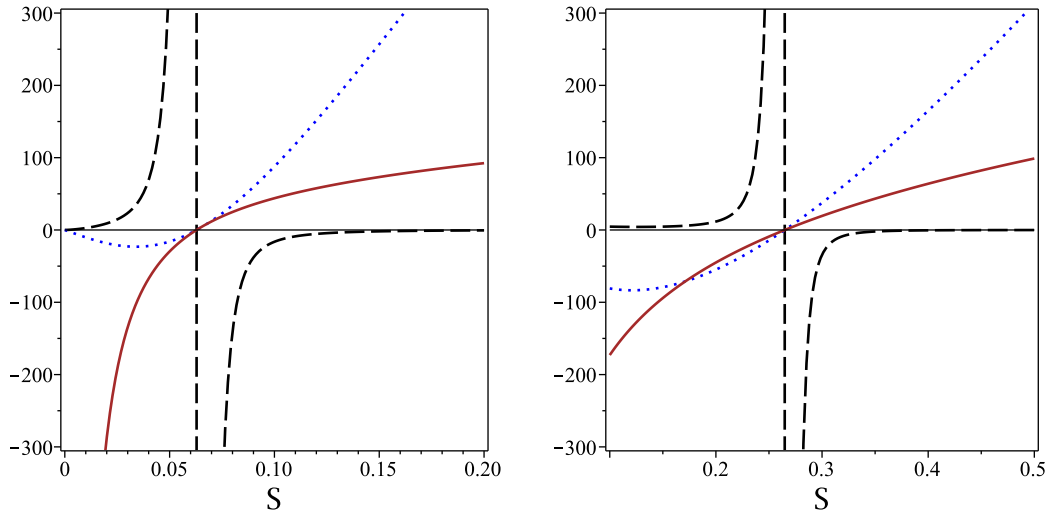


FIG. 3: T (continuous line), C_Q (dotted line) and $R_{HP\text{EM}}$ (dashed line) versus S for $Q = 0.02$, $\Lambda(\varepsilon) = -1$, $f(\varepsilon) = g(\varepsilon) = 1.1$. **Left diagram:** for $k = 0$. **Right diagram:** for $k = -1$.

Using the above equation, we obtain two divergence points for heat capacity (S_1^* and S_2^*) as

$$\begin{cases} S_1^* = \frac{-k + \sqrt{k^2 + 192\pi^2 \Lambda(\varepsilon) Q^2}}{8\Lambda(\varepsilon)} \\ S_2^* = \frac{-k - \sqrt{k^2 + 192\pi^2 \Lambda(\varepsilon) Q^2}}{8\Lambda(\varepsilon)} \end{cases}, \quad (31)$$

As one can see, our results show that, the phase transition critical points depend on topological factor (k), the cosmological constant ($\Lambda(\varepsilon)$) and also the total charge (Q). Here, we are going to investigate the behavior of the phase transition critical points in table (II) and figures 2-5.

According to the obtained results for phase transition critical points (or divergence points) in table (II) and figures 2-5, we may encounter with three different cases:

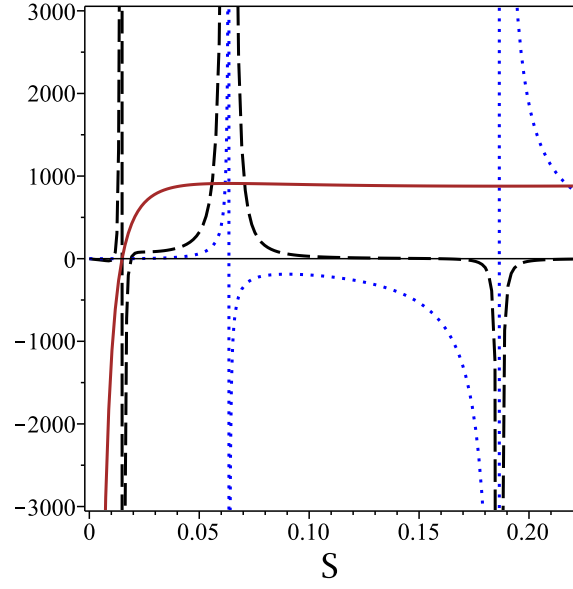


FIG. 4: T (continuous line), C_Q (dotted line) and R_{HPEM} (dashed line) versus S for $Q = 0.02$, $\Lambda(\varepsilon) = 1$, $f(\varepsilon) = g(\varepsilon) = 1.1$, $k = 1$.

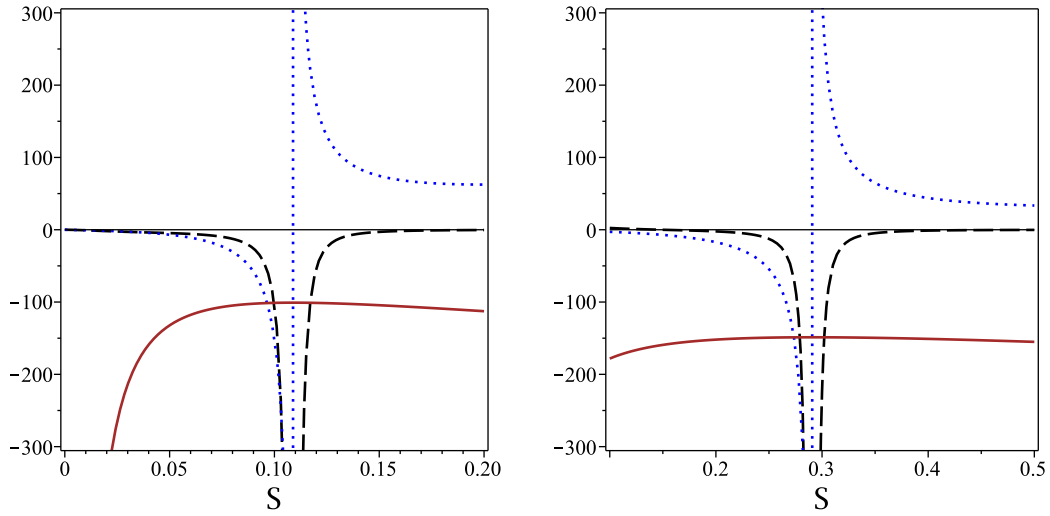


FIG. 5: T (continuous line), C_Q (dotted line) and R_{HPEM} (dashed line) versus S for $Q = 0.02$, $\Lambda(\varepsilon) = 1$, $f(\varepsilon) = g(\varepsilon) = 1.1$. **Left diagram:** for $k = 0$. **Right diagram:** for $k = -1$.

TABLE II: The phase transition critical points for $Q = 0.02$.

k	$\Lambda(\varepsilon)$	S_1^*	S_2^*	number of points
1	1	0.041	—	1
1	-1	0.063	0.186	2
0	1	0.109	—	1
0	-1	—	—	0
-1	1	0.291	—	1
-1	-1	—	—	0

Case I: there are two divergencies for the heat capacity (S_1^* and S_2^*). Since the black holes are physical and unstable between two divergencies (the temperature is positive but the heat capacity is negative), therefore, a phase transition from the black holes with small entropy (small black holes) to large entropy (large black holes) occurs between two divergencies (see Fig. 4). This phase transition is similar to the Van der Waals phase transition for black hole. It has been found that the thermodynamics of an asymptotically AdS metric in 4-dimensional spacetime matches exactly with the thermodynamics of the Van der Waals fluid. In other words, the isocharge in the temperature-entropy plane has an unstable branch and two stable ones when the charge below a critical value, and also there exists a second-order critical point at a critical charge. Therefore, for $k = 1$, we encounter with a Van der Waals-like phase transition of black hole in gravity's rainbow (see Fig. 4). Recently, the research on a Van der Waals-like phase transition has been generalized to the extended phase space [94–100]. In this framework, the cosmological constant is taken as a thermodynamical pressure ($P = -\frac{\Lambda}{8\pi}$), and its conjugate quantity is treated as the thermodynamical volume [51]. Considering this view, there is a precise pressure-volume oscillatory behavior and the small-large black hole phase transition is identified with the liquid-gas phase transition of the van der Waals fluid [101]. This feature has been investigated for black holes with more details in refs. [102–108].

Case II: existence of one divergency (S_1^*). In this case we encounter with two different cases which depend on the sign of temperature of black holes. First: there is a phase transition from the unstable black holes with large entropy to the stable black holes with small entropy (see Fig. 2). Second: there is no phase transition when the temperature is negative because the black holes are non-physical (see Fig. 5).

Case III: there is no divergence point. It is notable that, the maximum of temperature is where the system acquires divergency in its heat capacity. Therefore, the absence of divergency in the heat capacity is due to the fact that there is no the maximum for the temperature of black holes (see Fig. 3).

Another approach for studying the phase transition critical points of black holes is related to geometrical thermodynamics. There are several metrics that one can employ in order to build a geometrical phase space by thermodynamical quantities such as Weinhold [84, 85], Ruppeiner [86, 87], Quevedo [88, 89], and HPEM [90]. It was previously argued that Ruppeiner, Weinhold and Quevedo metrics may not provide us with a completely flawless mechanism for studying the geometrical thermodynamics of specific types of black holes (see Refs. [109–111], for more details). Therefore, in this paper, we consider the HPEM metric and investigate geometrical thermodynamics of topological charged black holes in gravity's rainbow.

The HPEM metric is given by [90]

$$dS_{HPEM}^2 = \frac{SM_S}{M_{QQ}^3} (-M_{SS}dS^2 + M_{QQ}dQ^2), \quad (32)$$

where $M_S = \left(\frac{\partial M(S,Q)}{\partial S}\right)_Q$, $M_{SS} = \left(\frac{\partial^2 M(S,Q)}{\partial S^2}\right)_Q$ and $M_{QQ} = \left(\frac{\partial^2 M(S,Q)}{\partial Q^2}\right)_S$. Calculations show that the numerator and denominator of Ricci scalar of HPEM metric (32), are given by the following forms

$$\begin{aligned} \text{numerator } (R_{HPEM}) &= S^2 M_S^2 M_{QQ}^3 M_{SSS} \left(\frac{M_{SS}}{M_S} - \frac{1}{S}\right) + S^2 M_S^2 M_{QQ}^3 M_{SQ} \left(2M_{SSS} + \frac{M_{SS}}{S} - \frac{M_{SS}^2}{M_S}\right) \\ &+ S^2 M_S^2 M_{SS}^2 M_{QQ}^2 \left(\frac{M_{SQ} M_{QQ}}{M_S M_{QQ}^2} - 9\right) + 6S^2 M_S^2 M_{QQ}^2 M_{SS}^2 \left(\frac{M_{QQ} M_{QQ}}{M_{QQ}} - \frac{M_{SS} M_{QQ}}{M_{SS}}\right) \\ &+ S^2 M_S^2 M_{SQ}^2 M_{SS}^2 M_{QQ}^2 \left(2 - \frac{M_S M_{SS} M_{SQ}}{M_{SS} M_S M_{SQ}}\right) + S^2 M_{QQ}^2 (M_S^2 M_{SS}^2 M_{SQ} - 2M_{SS}^3 M_{QQ}) \\ &+ S^2 M_S^2 M_{SS} M_{QQ} (2M_{SQ}^2 M_{QQ} + 4M_{QQ} M_{SS} M_{SQ}) - 2M_S^2 M_{SS} M_{QQ}^3, \end{aligned} \quad (33)$$

$$\text{denominator } (R_{HPEM}) = 2S^3 M_S^3 M_{SS}^2, \quad (34)$$

where $M_{XX} = \left(\frac{\partial^2 M}{\partial X^2}\right)$, $M_{XY} = \left(\frac{\partial^2 M}{\partial X \partial Y}\right)$, $M_{XXX} = \left(\frac{\partial^3 M}{\partial X^3}\right)$, $M_{XXXX} = \left(\frac{\partial^4 M}{\partial X^4}\right)$ and also $M_{XXYY} = \left(\frac{\partial^4 M}{\partial X^2 \partial Y^2}\right)$.

Our results show that, denominator of the Ricci scalar of the HPEM metric contains numerator and denominator of the heat capacity. In other words, divergence points of the Ricci scalar of HPEM metric coincide with both roots (the physical limitation points) and phase transition critical points of the heat capacity. Therefore, all the physical limitation and the phase transition critical points are included in the divergencies of the Ricci scalar of HPEM metric (see Figs. 2-5). Another important results of HPEM metric is related to the different behavior of Ricci scalar before and after its divergence points. It was seen that the behavior of Ricci scalar for divergence points related to the physical limitation and phase transition critical points is different. In other words, the sign of Ricci scalar change before and after divergencies when the heat capacity is zero (see figs. 2-4). But the signs of Ricci scalar are the same when the heat capacity encounter with divergencies (see figs. 2, 4 and 5). These divergencies called Λ divergencies.

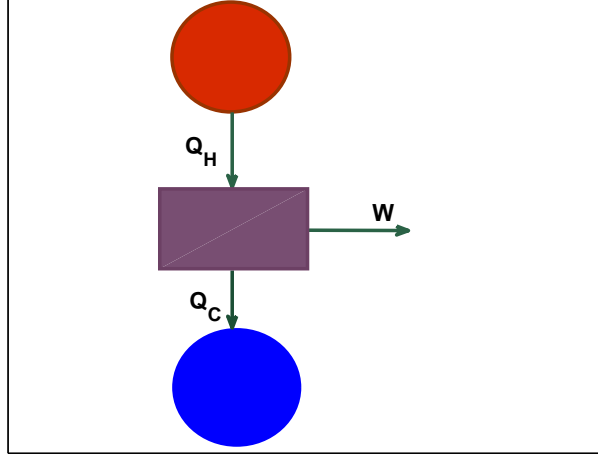


FIG. 6: The heat engine flows.

Therefore, considering this approach also enable us to distinguish physical limitation and phase transition critical points from one another.

V. HEAT EFFICIENCY

In this section, we are going to obtain another important quantity for black holes which is called the heat efficiency. In this paper, we are interested in classical heat engine. A heat engine is a physical system that takes heat from warm reservoir and turns a part of it into the work while its remaining is given to cold reservoir (see Fig. (6), for more details). In order to calculate work done by the heat engine and given the equation of state, one can use the $P - V$ diagrams for describing the heat engine which results into a closed path [66–68]. On the other hand, Wei and Liu showed the work or heat through measuring the areas by casting the process into the $T - S$ diagram, see Fig. 2 in ref. [69] for more details. It is notable that, for a thermodynamics cycle, one may extract mechanical work via the PdV term in the first law of thermodynamics as $W = Q_H - Q_C$ (the first law of thermodynamics is given as $\Delta U = \Delta Q - W$). According to this fact that ΔU (the internal energy changes) is zero for a thermodynamic cycle, the first law of thermodynamics reduces to $W = \Delta Q = Q_H - Q_C$, where Q_H is a net input heat flow, Q_C is a net output flow and also W is a net output work. On the other hand, the efficiency of heat engine is defined as

$$\eta = \frac{W}{Q_H} = \frac{Q_H - Q_C}{Q_H} = 1 - \frac{Q_C}{Q_H}, \quad (35)$$

The heat engine depends on the choice of path in the $P - V$ diagram and also the equation of state of the black hole in question. Some classical cycles such as Carnot cycle includes a pair of isotherms at temperatures T_H and T_C where $T_H > T_C$ (T_H and T_C are temperatures of the warm and the cold reservoirs, respectively), for this cycle, there is a pair of isotherms with different temperatures where cycle has maximum efficiency and it is described by $\eta = 1 - \frac{T_C}{T_H}$. It is noteworthy that for this case, there is an isothermal expansion where the system absorbs some heat and an isothermal compression during expulsion of some heat of the system. It is possible to show that these two paths of isotherms are connected to each other by different methods. The first method is using isochoric path, like classical Stirling cycle. The second one is adiabatic path similar to classical Carnot cycle. Therefore, the form of path is a key factor for the definition of cycle.

It is notable that the thermodynamic volume of topological black holes in gravity's rainbow is given as

$$V = \frac{r_+^3}{3f(\varepsilon)g^3(\varepsilon)}. \quad (36)$$

On the other hand, for the obtained black holes in this gravity, the entropy S and the thermodynamic volume V are related by Eqs. (18) and (36) as $S = \frac{r_+^2}{4g^2(\varepsilon)} = \frac{[3Vf(\varepsilon)]^{2/3}}{4}$. In other words, entropy depends on volume ($S \propto V$). It

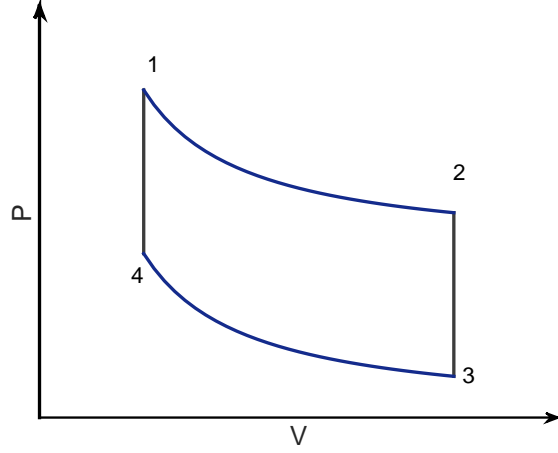


FIG. 7: Carnot cycle.

means that adiabatic and isochores are the same (Carnot and Stirling methods coincide with each other). Therefore, the efficiency of cycle can be calculated easily.

So along the upper isotherm (Fig. (7)) and by considering Eqs. (18) and (36), the net input heat flow is given as

$$Q_H = T_H \Delta S_{1 \rightarrow 2} = \frac{T_H}{4} (3f(\varepsilon))^{2/3} (V_2^{2/3} - V_1^{2/3}), \quad (37)$$

and also along the lower isotherm (Fig. (7)) and by considering Eqs. (18) and (36), the net output heat flow is given as

$$Q_C = T_C \Delta S_{3 \rightarrow 4} = \frac{T_C}{4} (3f(\varepsilon))^{2/3} (V_3^{2/3} - V_4^{2/3}), \quad (38)$$

which according to Fig. (7), we have $V_1 = V_4$ and $V_2 = V_3$, and by using the equation (35), the efficiency of heat engine becomes

$$\eta = 1 - \frac{Q_C}{Q_H} = 1 - \frac{T_C}{T_H}. \quad (39)$$

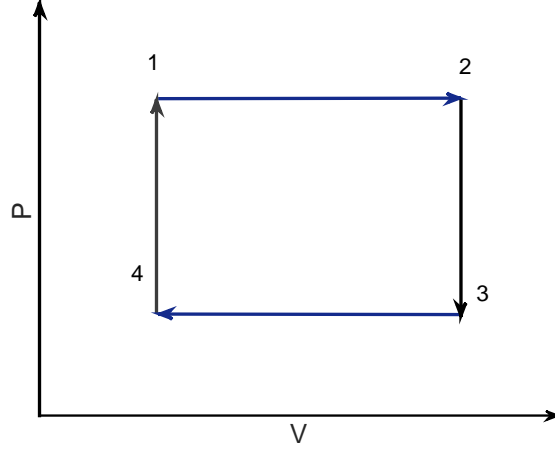
It is notable that, the heat engine for black holes was proposed by Johnson in 2014 [66]. Considering the concepts introduced by Johnson, the heat engines provided by black holes in various gravities have been investigated in some literatures. For example; the heat engine for Gauss-Bonnet [67], Born-Infeld AdS [70], dilatonic Born-Infeld [71], charged AdS black holes [72], Black hole in conformal gravity [73], Kerr AdS and dyonic black holes [74], BTZ [75], polytropic black holes [76], black holes in massive gravity [77] and Accelerating AdS black holes [78] have been studied (see refs. [79–82], for more details). Also, Wei and Liu suggested that the working substance is the fluid constituted with the virtual black hole molecules which carry the degree of freedom of black hole entropy [83]. Then they studied the black hole heat engine by a charged anti de Sitter black hole. In the reduced $T - S$ chart, it was found that the work, heat and efficiency of the engine are independent of the black hole charge. Also, their results showed that the black hole engine working along the Rankine cycle with a back pressure mechanism has a higher efficiency. Their results provided efficient mechanism to produce the useful mechanical work with black hole and such heat engine may act as a possible energy source for the high energy astrophysical phenomena near the black hole [69].

Here, we want to obtain the efficiency of heat engine for topological black holes in gravity's rainbow. For this purpose, by inserting $\Lambda(\varepsilon) = -8\pi P$ in the obtained temperature of black holes (Eq. (17)), we have

$$T = \frac{1}{4\pi} \left(\frac{kg(\varepsilon)}{f(\varepsilon)r_+} + \frac{8\pi Pr_+}{f(\varepsilon)g(\varepsilon)} \right). \quad (40)$$

Solving the equation (40), we obtain the pressure in the following form

$$P = \frac{g(\varepsilon)}{8\pi r_+^2} (4\pi r_+ f(\varepsilon) T - kg(\varepsilon)). \quad (41)$$

FIG. 8: P - V diagram.

There are two different heat capacities for a system; the heat capacity at constant pressure (C_P) and the heat capacity at constant volume (C_V). The heat capacities at constant pressure and at constant volume can be calculated by the standard thermodynamic relations, as

$$C_V = T \frac{\partial S}{\partial T} \Big|_V, \quad (42)$$

$$C_P = T \frac{\partial S}{\partial T} \Big|_P. \quad (43)$$

According to this fact that the entropy of black holes in gravity's rainbow is a regular function of the thermodynamic volume V ($S \propto V$), the heat capacity at constant volume will vanish, $C_V = 0$. Therefore an explicit expression for C_P would suggest that there should be a new engine which includes two isobars and two isochores/adiabatic similar to Fig. 8.

For this purpose, we can consider a rectangle cycle in the $P - V$ plane (Fig. 8) which consists two isobars (paths of $1 \rightarrow 2$ and $3 \rightarrow 4$) and two isochores (paths of $2 \rightarrow 3$ and $4 \rightarrow 1$). Also, a possible scheme for this heat engine involves specifying values of temperature where $T_2 = T_H$ and $T_4 = T_C$. According to the fact that the paths of $1 \rightarrow 2$ and $3 \rightarrow 4$ are isobars, we find $P_1 = P_2$ and $P_3 = P_4$. So, we can calculate the work which is done in this cycle as

$$\begin{aligned} W &= \oint P dV = W_{1 \rightarrow 2} + W_{2 \rightarrow 3} + W_{3 \rightarrow 4} + W_{4 \rightarrow 1} \\ &= W_{1 \rightarrow 2} + W_{3 \rightarrow 4} = (P_1 - P_4)(V_2 - V_1). \end{aligned} \quad (44)$$

It is notable that the works which are done in the paths of $2 \rightarrow 3$ and $4 \rightarrow 1$ are isochores, therefore, these terms are zero.

On the other hand, C_P for these black holes is calculated as

$$C_P = T \frac{\partial S}{\partial T} \Big|_P = T \frac{\left(\frac{\partial S}{\partial r_+} \right)}{\left(\frac{\partial T}{\partial r_+} \right)} = \frac{(8\pi r_+^2 f(\varepsilon) T + k g^2(\varepsilon)) r_+^2}{2g^2(\varepsilon) (8\pi r_+^2 P - k g^2(\varepsilon))}. \quad (45)$$

Here, we want to consider the large temperature limit ($T \gg 0$). In other words, we can discard the terms in which the temperature are in the denominator, i. e. $\frac{1}{T}$, $\frac{1}{T^2}$, ... have small values. In this paper, we keep the term, $\frac{1}{T}$, and omit higher orders of T ($\frac{1}{T^2}$, ...) in order to extract r_+ from the equation (40) resulting into

$$r_+ = \frac{f(\varepsilon) g(\varepsilon) T}{2P} - \frac{k g(\varepsilon)}{4\pi f(\varepsilon) T} + \dots, \quad (46)$$

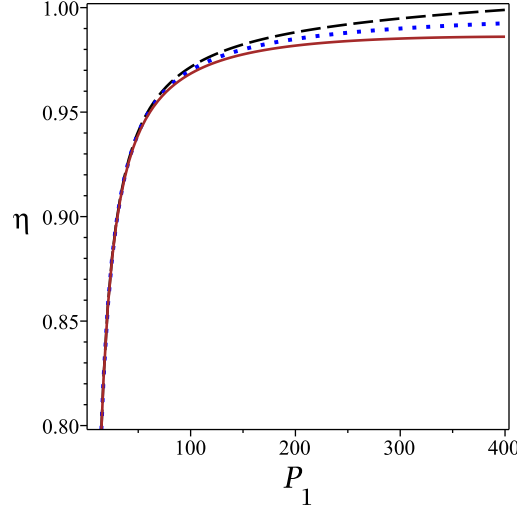


FIG. 9: η versus P_1 for $T_2 = 100$, $T_1 = 80$, $P_4 = 3$, $f(\epsilon) = 1.1$, $k = -1$ (dashed line), $k = 0$ (dotted line) and $k = 1$ (continuous line).

which by inserting the above equation in the thermodynamic volume (36) and the heat capacity (45), we obtain V and C_P as

$$V = \frac{r_+^3}{3f(\epsilon)g^3(\epsilon)} = \frac{f^2(\epsilon)T^3}{24P^3} - \frac{kT}{16\pi P^2} + \dots, \quad (47)$$

$$C_P = \frac{f^2(\epsilon)T^2}{8P^2} + \dots. \quad (48)$$

Now, we are in a position to obtain the heat input and the work done by the heat engine

$$Q_H = \int_{T_1}^{T_2} C_P dT = \frac{f^2(\epsilon)}{24P_1^2} (T_2^3 - T_1^3) + \dots, \quad (49)$$

$$W = (P_1 - P_4)(V_2 - V_1) = \left(1 - \frac{P_4}{P_1}\right) \left(\frac{f^2(\epsilon)(T_2^3 - T_1^3)}{24P_1^2} - \frac{k(T_2 - T_1)}{16\pi P_1} + \dots \right). \quad (50)$$

As one can see, the heat input depends on rainbow function ($f^2(\epsilon)$). Also, the work done by the heat engine (W) depends on both rainbow function ($f^2(\epsilon)$) and topological factor (k).

After some calculation, the engine efficiency is given as

$$\eta = \frac{W}{Q_H} = \left(1 - \frac{P_4}{P_1}\right) \left[1 - \frac{3kP_1}{2\pi f^2(\epsilon)(T_1^2 + T_1T_2 + T_2^2)} + \dots \right]. \quad (51)$$

In order to have positive efficiency and this fact that the efficiency satisfies the relation $\eta \leq 1$, we obtain the following condition for topological factor as

$$k < \frac{2\pi f^2(\epsilon)(T_1^2 + T_1T_2 + T_2^2)}{3P_1}. \quad (52)$$

Our results show that the rainbow function and the topological factor affect efficiency. Considering that the horizon of black hole in gravity's rainbow could be sphere, flat or hyperbolic, corresponding to $k = 1$; 0 or -1 , respectively, we want to study the effects this factor on the engine's efficiency. We found that the efficiency of black hole engines in this gravity with hyperbolic horizon ($k = -1$) is higher than that of black holes with flat horizon ($k = 0$). Also, one finds that the spherical black holes ($k = 1$) have the lowest efficiency. In other words, $\eta_{k=-1} > \eta_{k=0} > \eta_{k=1}$. In order to have more details, we plot Figs. 9, 10 and 11.

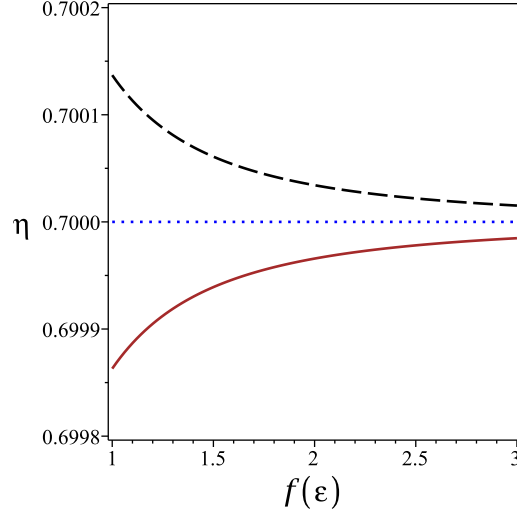


FIG. 10: η versus $f(\epsilon)$ for $T_2 = 100$, $T_1 = 80$, $P_1 = 10$, $P_4 = 3$, $k = -1$ (dashed line), $k = 0$ (dotted line) and $k = 1$ (continuous line).

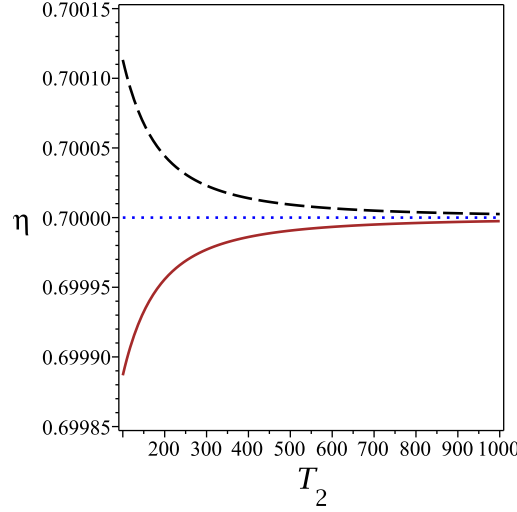


FIG. 11: η versus T_2 for $T_1 = 80$, $P_1 = 10$, $P_4 = 3$, $f(\epsilon) = 1.1$, $k = -1$ (dashed line), $k = 0$ (dotted line) and $k = 1$ (continuous line).

The Fig. 9, show that the efficiency (η) will monotonously increase with the growth of pressure P_1 . In other words η will approach to the maximum efficiency, i.e. the Carnot efficiency is allowed by thermodynamics laws. In the high pressure limit (P^*), we have

$$\lim_{P_1 \rightarrow P^*} \eta = 1. \quad (53)$$

Another interesting result is related to the effects of rainbow function. According to this fact that the rainbow function ($f^2(\epsilon)$) located in the denominator of the second term of Eq. (51), therefore by increasing the value of rainbow function (or by increasing the effects of gravity's rainbow), the engine efficiency decreases. In the absence of gravity's rainbow ($f^2(\epsilon) = 1$), the effects of topological factor on engine efficiencies are clear, but by considering large quantities of rainbow function more than one ($f(\epsilon) > 1$), the behavior of engine efficiencies for topological black holes are the same (see Fig. (10)). Also, there is the same behavior for high temperature (see Fig. (11)). In other words, for $T_2 \gg T_1$, the engine's efficiencies for topological black holes are the same, but for T_2 near to T_1 ($T_2 \simeq T_1$), the differences are clear.

VI. CLOSING REMARKS

In this paper, we considered gravity's rainbow in order to include UV limit in general relativity. First, we obtained solutions and showed that these solutions may be interpreted as black holes with two horizons, extreme black hole (one horizon) or naked singularity (without horizon). It is notable that, the dependency of all constants on energy functions was considered. The asymptotical behavior of obtained solutions was energy dependent (a)dS. Then, we calculated thermodynamic and conserved quantities for these black holes and showed that these quantities depend on rainbow functions, $(f(\varepsilon)$ and $g(\varepsilon))$, and satisfy the first law of thermodynamics.

Next, we conducted a study regarding physical/nonphysical black holes (positivity/negativity of temperature) and thermal stability of the solutions. Our results showed that the physical limitation points depend on topological factor (k), the modified cosmological constant ($\Lambda(\varepsilon)$) and also the total charge (Q). We found that these black holes could have three different behaviors;

(i) two roots for the temperature and the heat capacity, so that, the obtained black holes were physical and enjoy thermal stability when their entropy are in range $S_1 < S < S_{div}$ (where S_1 and S_{div} are first root and divergency point).

(ii) one root or a critical entropy, S_1 . Here, we come across two different situations. In this case, we faced with physical and stable topological charged black holes when entropy was bigger than critical entropy ($S > S_1$).

(iii) no root. In this case, the obtain black holes were non-physical.

In order to study the phase transition critical points or divergence points, we investigated denominator of the heat capacity. We found that there were three different cases available for these black hole:

(i) two divergencies (S_1^* and S_2^*). There was a phase transition between the black holes with small entropy (or small black holes) to large entropy (or large black holes) and vice versa. This phase transition is related to first order transition.

(ii) one divergency (S_1^*). In this case, we encountered with two different cases. *CaseI*: existence of a phase transition from the unstable black holes with large entropy to the stable black holes with small entropy. *CaseII*: no phase transition.

(iii) no divergency.

In addition, we used the geometrical thermodynamics for studying both the physical limitation and phase transition critical points of topological charged black holes in gravity's rainbow. It was shown that the divergencies of the curvature scalar of the HPEM metric exactly coincide with both the physical limitation and phase transition critical points of system. In other words, the divergencies of heat capacity and its root are matched with the divergencies of Ricci scalar. It is worthwhile to mention that the behavior of Ricci scalar around its divergence points for roots and phase transition critical points were different. It means that there were characteristic behaviors that enable one to recognize the divergence point of Ricci scalar related to the root of heat capacity or temperature (in this case the divergencies around the physical limitation points were from positive infinity to negative infinity and vice versa) from the divergence points of Ricci scalar related to the divergencies of heat capacity (in this case the divergencies around phase transition critical points were similar to Λ which called Λ divergencies). Therefore, one is able to point out that a physical limitation and phase transition critical points occurred in the divergencies of thermodynamical Ricci scalar of the HPEM metric with different distinctive behaviors.

Finally, by considering the heat engine for black hole which was proposed by Johnson, we studied the efficiency of heat engines for topological black holes in gravity's rainbow. We found that the efficiency of heat engine depends on topological factor and rainbow function ($f(\varepsilon)$). We extracted some interesting results about the efficiency of heat engines for these black holes as;

(i) the efficiency for black holes with hyperbolic horizon was bigger than that of black holes with flat horizon ($k = 0$), and the spherical black holes ($k = 1$) had the lowest efficiency ($\eta_{k=-1} > \eta_{k=0} > \eta_{k=1}$).

(ii) with increasing pressure P_1 , the efficiency reach to the maximum efficiency, i.e. the Carnot efficiency is allowed by thermodynamics laws. In fact, in the high pressure limit (P^*), $\lim_{P_1 \rightarrow P^*} \eta = 1$.

(iii) in the absence of gravity's rainbow ($f(\varepsilon) = 1$), the effects of topological factor on engine's efficiencies were diffident, but for the large values of rainbow function ($f(\varepsilon) > 1$), the behavior of engine's efficiencies for different topological black holes were the same.

(iv) for $T_2 \gg T_1$, the engine's efficiencies for different topological black holes were the same, but for T_2 near to T_1 ($T_2 \simeq T_1$), the differences were clear.

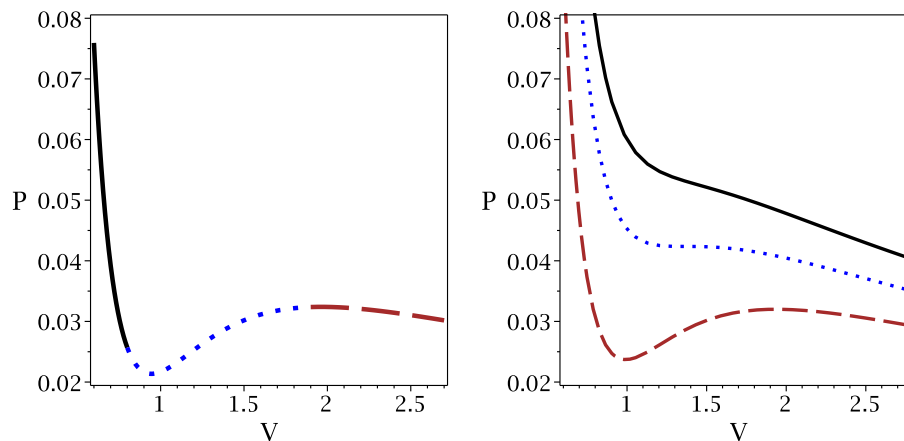


FIG. 12: **Left panel:** $P - V$ diagram for $T < T_c$.

Right panel: $P - V$ diagrams for $T > T_c$ (continuous line), $T = T_c$ (dotted line) and $T < T_c$ (dashed line).

Acknowledgments

This work has been supported financially by Research Institute for Astronomy and Astrophysics of Maragha (RI-AAM) under research project No. 1/5440-22.

Appendix: phase transition and the heat engine efficiency

Here, we are going to give more information about $P - V$ diagram of a black hole in different temperature. We have two cases for different temperature in Fig. 12.

Case I: left panel of Fig. 12 shows that there are three areas for black holes which encounter with a phase transition when $T \leq T_c$ (T_c is critical temperature). The first area is related to high pressure (continuous line in left panel in Fig. (12)). The black hole in this area has small radius and it is called small black hole (SBH) region. The second area is related to unstable phase (dotted line in left panel in Fig. (12)). The third area is related to low pressure case (dashed line in left panel of Fig. (12)). In this area, black holes have large radius, and it is known as large black hole (LBH) region.

Case II: for the temperatures more than critical temperature ($T > T_c$), the phase transition and the second area are disappeared (see right panel of Fig. (12) for more details). In phase transition point, the transition takes place between SBH to LBH. The opposite could also take place in the case black holes horizon shrinking (the LBH to the SBH).

In this work we considered the high temperature for investigating heat engine of black hole in gravity's rainbow. Depending to the critical temperature of our system, this temperature may include phase transition area in the $P - V$ plane or not.

In addition, the relation between the heat engine efficiency and $T - S$ diagram have been evaluated in ref. [69].

-
- [1] D. Lovelock, J. Math. Phys. 12 (1971) 498.
 - [2] D. Lovelock, J. Math. Phys. 13 (1972) 874.
 - [3] P. Brax and C. van de Bruck, Class. Quantum Grav. 20 (2003) R201.
 - [4] L. A. Gergely, Phys. Rev. D 74 (2006) 024002.
 - [5] C. Brans and R. H. Dicke, Phys. Rev. 124 (1961) 925.
 - [6] R. G. Cai and Y. S. Myung, Phys. Rev. D 56 (1997) 3466.
 - [7] J. C. C. de Souza and V. Faraoni, Class. Quantum Grav. 24 (2007) 3637.
 - [8] G. Cognola, E. Elizalde, S. Nojiri, S. D. Odintsov, L. Sebastiani and S. Zerbini, Phys. Rev. D 77 (2008) 046009.
 - [9] T. P. Sotiriou and V. Faraoni, Rev. Mod. Phys. 82 (2010) 451.
 - [10] S. Nojiri, S. D. Odintsov and V. K. Oikonomou, Phys. Rept. 692 (2017) 1.
 - [11] M. Fierz and W. Pauli, Proc. Roy. Soc. Lond. A 173 (1939) 211.
 - [12] E. A. Bergshoeff, O. Hohm and P. K. Townsend, Phys. Rev. Lett. 102 (2009) 201301.
 - [13] C. de Rham, G. Gabadadze and A. J. Tolley, Phys. Rev. Lett. 106 (2011) 231101.

- [14] J. Magueijo and L. Smolin, *Phys. Rev. Lett* 88 (2002) 190403.
- [15] J. Magueijo and L. Smolin, *Class. Quantum Grav.* 21 (2004) 1725.
- [16] G. Amelino-Camelia, *Phys. Lett. B* 510 (2001) 255.
- [17] G. Amelino-Camelia and J. Kowalski-Glikman, *Phys. Lett. B* 522 (2001) 133.
- [18] J. Kowalski-Glikman, *Phys. Lett. A* 286 (2001) 391.
- [19] G. Amelino-Camelia, *Nature* 418 (2002) 34.
- [20] J. J. Peng and S. Q. Wu, *Gen. Relativ. Gravit.* 40 (2008) 2619.
- [21] A. F. Ali, M. Faizal and B. Majumder, *Europhys. Lett.* 109 (2015) 20001.
- [22] Y. Gim and W. Kim, *JCAP* 05 (2015) 002.
- [23] A. F. Ali, M. Faizal and M. M. Khalil, *Phys. Lett. B* 743 (2015) 295.
- [24] A. F. Ali, *Phys. Rev. D* 89 (2014) 104040.
- [25] A. Awad, A. F. Ali and B. Majumder, *JCAP* 10 (2013) 052.
- [26] G. Santos, G. Gubitosi and G. Amelino-Camelia, *JCAP* 08 (2015) 005.
- [27] S. H. Hendi, M. Momennia, B. Eslam Panah and M. Faizal, *Astrophys. J.* 827 (2016) 153.
- [28] M. Khodadi, K. Nozari and H. R. Sepangi, *Gen. Rel. Grav.* 48 (2016) 166.
- [29] M. Khodadi, Y. Heydarzade, K. Nozari and F. Darabi, *Eur. Phys. J. C* 75 (2015) 590.
- [30] S. H. Hendi, G. H. Bordbar, B. Eslam Panah and S. Panahiyan, *JCAP* 09 (2016) 013.
- [31] B. Eslam Panah, G. H. Bordbar, S. H. Hendi, R. Ruffini, Z. Rezaei and R. Moradi, *Astrophys. J.* 848 (2017) 24.
- [32] H. L. Liu and G. L. Lü, [arXiv:1805.00333].
- [33] R. Garattini and G. Mandanici, *Eur. Phys. J. C* 77 (2017) 57.
- [34] R. Garattini and G. Mandanici, [arXiv:1601.00879].
- [35] R. Garattini and E. N. Saridakis, *Eur. Phys. J. C* 75 (2015) 343.
- [36] Y. Ling, X. Li and H. Zhang, *Mod. Phys. Lett. A* 22 (2007) 2749.
- [37] J. -J. Peng and S. -Q. Wu, *Gen. Rel. Grav.* 40 (2008) 2619.
- [38] C. Leiva, J. Saavedra and J. Villanueva, *Mod. Phys. Lett. A* 24 (2009) 1443.
- [39] S. Gangopadhyay and A. Dutta, *Euro. Phys. Lett.* 115 (2016) 50005.
- [40] S. Alsaleh, *Eur. Phys. J. Plus* 132 (2017) 181.
- [41] Y. -W. Kim, S. K. Kim and Y. -J. Park, *Eur. Phys. J. C* 76 (2016) 557.
- [42] Z. -W. Feng, and S. -Z. Yang, *Phys. Lett. B* 772 (2017) 737.
- [43] G. Alencar, R. N. Costa Filho, M. S. Cunha and C. R. Muniz, [arXiv:1805.01791].
- [44] R. Garattini, *JCAP* 06 (2013) 017.
- [45] S. H. Hendi, B. Eslam Panah, S. Panahiyan and M. Momennia, *Adv. High Energy Phys.* 2016 (2016) 9813582.
- [46] S. H. Hendi, B. Eslam Panah and S. Panahiyan, *Phys. Lett. B* 769 (2017) 191.
- [47] S. H. Hendi and M. Faizal, *Phys. Rev. D* 92 (2015) 044027.
- [48] S. H. Hendi, H. Behnamifard and B. Bahrani-Asl, *PTEP* 2018 (2018) 033E03.
- [49] S. H. Hendi, A. Dehghani and M. Faizal, *Nucl. Phys. B* 914 (2017) 117.
- [50] S. H. Hendi, M. Faizal, B. Eslam Panah and S. Panahiyan, *Eur. Phys. J. C* 76 (2016) 296.
- [51] B. P. Dolan, *Class. Quantum Grav.* 28 (2011) 125020.
- [52] B. P. Dolan, *Class. Quantum Grav.* 28 (2011) 235017.
- [53] D. Grumiller, R. McNees and J. Salzer, *Phys. Rev. D* 90 (2014) 044032.
- [54] B. P. Dolan, *JHEP* 10 (2014) 179.
- [55] D. Kastor, S. Ray and J. Traschen, *JHEP* 11 (2014) 120.
- [56] A. Karch and B. Robinson, *JHEP* 12 (2015) 073.
- [57] E. Caceres, P. H. Nguyen and J. F. Pedraza, *JHEP* 09 (2015) 184.
- [58] Z. Y. Nie and H. Zeng, *JHEP* 10 (2015) 047.
- [59] X. -X. Zeng and L. -F. Li, *Phys. Lett. B* 764 (2017) 100.
- [60] D. Kastor, S. Ray and J. Traschen, *Class. Quant. Grav.* 26 (2009) 195011.
- [61] D. Kubiznak and R. B. Mann, *JHEP* 07 (2012) 033.
- [62] S. Gunasekaran, R. B. Mann and D. Kubiznak, *JHEP* 11 (2012) 110.
- [63] N. Altamirano, D. Kubiznak and R. B. Mann, *Phys. Rev. D* 88 (2013) 101502.
- [64] N. Altamirano, D. Kubiznak, R. B. Mann and Z. Sherkatghanad, *Class. Quant. Grav.* 31 (2014) 042001.
- [65] S. -W. Wei and Y. -X. Liu, *Phys. Rev. D* 90 (2014) 044057.
- [66] C. V. Johnson, *Class. Quantum Grav.* 31 (2014) 205002.
- [67] C. V. Johnson, *Class. Quantum Grav.* 33 (2016) 215009.
- [68] C. V. Johnson, *Entropy*, 18 (2016) 120.
- [69] S. -W. Wei and Y. -X. Liu, [arXiv:1605.04629].
- [70] C. V. Johnson, *Class. Quantum Grav.* 33 (2016) 135001.
- [71] C. Bhamidipati and P. Kumar Yerra, *Eur. Phys. J. C* 77 (2017) 534.
- [72] H. Liu and X. -H. Meng, *Eur. Phys. J. C* 77 (2017) 556.
- [73] H. Xu, Y. Sun and L. Zhao, *Int. J. Mod. Phys. D* 26 (2017) 1750151.
- [74] J. Sadeghi and Kh. Jafarzade, *Int. J. Theor. Phys.* 56 (2017) 3387.
- [75] J. -X. Mo, F. Liang and G. -Q. Li, *JHEP* 03 (2017) 010.
- [76] M. R. Setare and H. Adami, *Gen. Relativ. Gravit.* 47 (2015) 133.
- [77] S. H. Hendi, B. Eslam Panah, S. Panahiyan, H. Liu and X. -H. Meng, *Phys. Lett. B* 781 (2018) 40.

- [78] J. Zhang, Y. Li and H. Yu, *Eur. Phys. J. C* 78 (2018) 645.
- [79] A. Chakraborty and C. V. Johnson, [arXiv:1612.09272].
- [80] R. A. Hennigar, F. McCarthy, A. Ballon and R. B. Mann, *Class. Quantum Grav.* 34 (2017) 175005.
- [81] F. Rosso, [arXiv:1801.07425].
- [82] J. -X. Mo and S. -Q. Lan [arXiv:1803.02491].
- [83] S. -W. Wei and Y. -X. Liu, *Phys. Rev. Lett.* 115 (2015) 111302.
- [84] F. Weinhold, *J. Chem. Phys.* 63 (1975) 2479.
- [85] F. Weinhold, *J. Chem. Phys.* 63 (1975) 2484.
- [86] G. Ruppeiner, *Phys. Rev. A* 20 (1979) 1608.
- [87] G. Ruppeiner, *Rev. Mod. Phys.* 67 (1995) 605.
- [88] H. Quevedo, *Gen. Relativ. Gravit.* 40 (2008) 971.
- [89] H. Quevedo and A. Sanchez, *JHEP* 09 (2008) 034.
- [90] S. H. Hendi, S. Panahiyan, B. Eslam Panah and M. Momennia, *Eur. Phys. J. C* 75 (2015) 507.
- [91] S. W. Hawking, *Commun. Math. Phys.* 43 (1975) 199.
- [92] S. W. Hawking, *Phys. Rev. D* 13 (1976) 191.
- [93] J. D. Beckenstein, *Phys. Rev. D* 7 (1973) 2333.
- [94] D. Kastor, S. Ray, J. Traschen, *Class. Quantum Grav.* 26 (2009) 195011.
- [95] S. H. Hendi and M. H. Vahidinia, *Phys. Rev. D* 88 (2013) 084045.
- [96] A. M. Frassino, D. Kubiznak, R. B. Mann and F. Simovic, *JHEP* 09 (2014) 080.
- [97] R. A. Hennigar and R. B. Mann, *Entropy* 17 (2015) 8056.
- [98] S. -W. Wei and Y. -X. Liu, *Phys. Rev. D* 91 (2015) 044018.
- [99] T. Delsate and R. Mann, *JHEP* 02 (2015) 070.
- [100] S. H. Hendi, R. B. Mann, S. Panahiyan and B. Eslam Panah, *Phys. Rev. D* 95 (2017) 021501(R).
- [101] D. Kubiznak and R. B. Mann, *JHEP* 07 (2012) 033.
- [102] S. -W. Wei, B. Liang and Y. -X. Liu, *Phys. Rev. D* 96 (2017) 124018.
- [103] D. -C. Zou, Y. Liu and R. Yue, *Eur. Phys. J. C* 77 (2017) 365.
- [104] S. H. Hendi, B. Eslam Panah, S. Panahiyan and M. Momennia, *Eur. Phys. J. C* 77 (2017) 647.
- [105] K. Bhattacharya, B. R. Majhi and S. Samanta, *Phys. Rev. D* 96 (2017) 084037.
- [106] M. Cadoni, E. Franzin and M. Taveri, *Phys. Lett. B* 768 (2017) 393.
- [107] S. H. Hendi, B. Eslam Panah and S. Panahiyan, *Fortschr. Phys.* 66 (2018) 1800005.
- [108] H. -L. Li and Z. -W. Feng, *Eur. Phys. J. C* 78 (2018) 49.
- [109] S. H. Hendi, S. Panahiyan and B. Eslam Panah, *Adv. High Energy Phys.* 2015 (2015) 743086.
- [110] S. H. Hendi and R. Naderi, *Phys. Rev. D* 91 (2015) 024007.
- [111] S. H. Hendi, S. Panahiyan, B. Eslam Panah and Z. Armanfard, *Eur. Phys. J. C* 76 (2016) 396.